BENEFITS FROM THE USE OF WIRE-COIL INSERTS IN WATER TRANSITIONAL AND LOW TURBULENT FLOW
The Influence of the Wire-Coil Pitch

by

Ventsislav ZIMPAROV [a], ***Plamen BONEV*** [a], ***Milcho ANGELOV*** [b], ***and Jordan HRISTOV*** [c*]

[a] Department of Mechanical Engineering, Gabrovo Technical University, Gabrovo, Bulgaria
[b] Technical Faculty, University of Food Technologies, Plovdiv, Bulgaria
[c] Department of Chemical Engineering, University of Chemical Technology and Metallurgy, Sofia, Bulgaria

Original scientific paper
https://doi.org/10.2298/TSCI211206060Z

Five wire-coil inserts with fixed wire diameter and different pitches, fitted inside a round tube have been experimentally studied in a transitional and low turbulent flow. Water was used as a working fluid at a wide range of flow conditions: $10^3 < Re < 10^4$ and $3.9 < Pr < 10.0$. The geometrical parameters of the inserts are: $e/D_i = 0.070$, and $p/e = 6.7$, 9.0, 10.0, 12.5, and 15.0. The variation of the friction factor and heat transfer coefficients have been obtained and compared with those of the smooth pipe. Performance evaluation criteria for the cases FG-1a, FG-2a, and VG-2a have been used to evaluate the maximum and real benefit that can be obtained. The greatest benefit can be achieved with the pitch of the wire-coil insert $p/e = 10.0$.

Key words: *heat transfer enhancement, transitional and low turbulent flow, pitch of wire-coil insert, benefits.*

Introduction

There are many heat exchangers provided with smooth tubes and fluids such as water that operate in transitional or low turbulent flow regimes. These heat exchangers are very appropriate to implement some heat transfer enhancement techniques such as wire coils or twisted tapes to improve the thermodynamic behaviour of the tube-side in single-phase transitional and low turbulent flow, Webb and Kim [1]. Wire-coil inserts possess some advantages compared to other techniques since they allow an easy and low cost installation in an existing heat exchanger with smooth tubes. The experimental works on heat transfer enhancement in transitional and low turbulent flow using wire-coil inserts, however, are not so much, Garcia *et al.* [2, 3], Martinez *et al.* [4].

The liquid solar collectors are also potential candidates for enhancing heat transfer, but only a few studies have been focused on [5-9], since most of the previous studies have been performed with twisted tapes as inserted devices. As Garcia *et al.* [2, 3] mentioned, the wire coils are especially suitable for enhancing heat transfer in the low turbulent and laminar flow domain, close to the operating flow rate in flat-plate solar collectors [10].

[*] Corresponding author, e-mail: hristovmeister@gmail.com

Garcia *et al.* [11] reported an experimental study on the use of wire-coil inserts to enhance heat transfer in typical flat-plate solar water collectors using wire-coil inserts for a wide range of operating conditions (different mass-flow rates and temperatures). The geometrical parameters of the wire coils are chosen according to the best thermodynamic behavior as observed in their previous works [2, 3], namely $e/D_\mathrm{i} = 0.072$, and $p/e = 13.9$.

The purpose of this research is to extend the study of Garcia *et al.* [2] towards the use of wire-coil inserts with smaller p/e than those examined by Garcia *et al.* [2], *i.e.*, $p/e < 15.0$, and find out the optimal value of p/e for which the greatest real benefit can be obtained.

Experiments and data reduction

Details of the experimental program, set-up design (counter-current water flow double-pipe heat exchanger), and verification of the results have been presented in Zimparov *et al.* [12-14]. The geometrical parameters of the smooth tube and the wire coils under study are presented in tab. 1, with the ratios e/D_i, p/e, and p/D_i.

Table 1. Geometrical parameters of the smooth tube and wire-coil inserts

D_i [mm]	p [mm]	e [mm]	p/e [–]	e/D_i [–]	p/D_i [–]
14.30	15.0	1.0	15.0	0.070	1.049
14.30	12.5	1.0	12.5	0.070	0.874
14.30	10.0	1.0	10.0	0.070	0.699
14.30	9.0	1.0	9.0	0.070	0.629
14.30	6.7	1.0	6.7	0.070	0.469

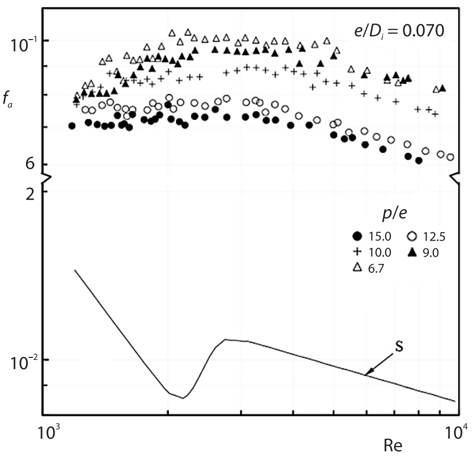

Figure 1. The variation of friction factor with Re

Figure 1 presents the variation of the average values of f_a with Reynolds number, together with the curve of f_s for the smooth pipe (noted with s). It is obvious that f_a depends on p/e and Reynolds number, but in a different way in the ranges $10^3 < \mathrm{Re} < 3\cdot10^3$, and $\mathrm{Re} > 3\cdot10^3$. In the range $10^3 < \mathrm{Re} < 3\cdot10^3$, two different correlations can be derived. The performance of each correlation has been assessed by the root mean square (RMS) deviation.

The two correlations are: eq. (1) and fig. 2:

$$f_\mathrm{a} = 0.0219\left(p/e\right)^{-0.198}\mathrm{Re}^{0.248}, \quad 6.7 < p/e < 9.0 \tag{1}$$

with RMS deviation of 6.7%. The relative deviations of all 44 experimental points from the correlation, eq. (1), are in the range ±10%, and eq. (2), fig. 3:

$$f_\mathrm{a} = 0.128\left(p/e\right)^{-0.402}\mathrm{Re}^{0.067}, \ 10.0 < p/e < 15.0 \tag{2}$$

with RMS deviation of 2.2%. The relative deviations of all 58 experimental points from the correlation, eq. (2), are in the range ±5%.

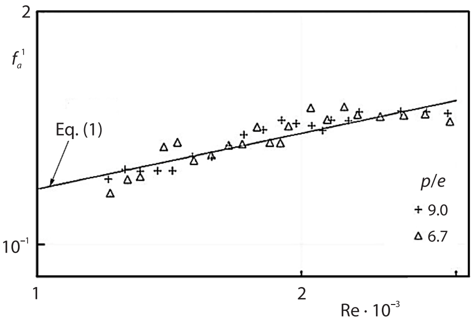

Figure 2. The variation of $f^1_a = f_a(p/e)^{0.198}$ with Re

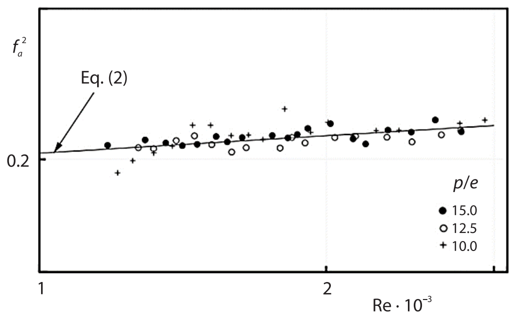

Figure 3. The variation of $f^2_a = f_a(p/e)^{0.402}$ with Re

For Re > $3\cdot10^3$, the variation of f_a can be presented by one correlation, eq. (3), fig. 4, with RMS deviation of 4.4%. The relative deviations of all 76 experimental points from the correlation, eq. (3), are in the range ±8%:

$$f_a = 1.183\left(p/e\right)^{-0.422}\,\mathrm{Re}^{-0.199} \qquad 6.7 \le p/e \le 15.0 \tag{3}$$

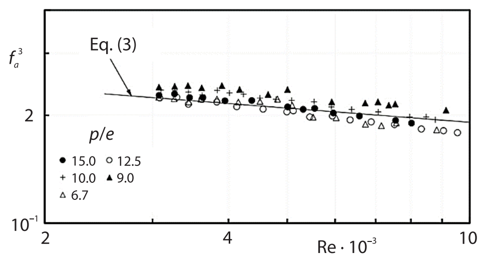

Figure 4. The variation of $f^3_a = f_a(p/e)^{0.422}$ with Re

Figure 5 shows the variation of friction factor augmentation ratio $f_* = f_a/f_s$ with Reynolds number. The tendency of the friction factor behaviour is very clearly expressed in this figure, and it confirms that of other studies, Garcia *et al.* [2], Vicente *et al.* [15], and Olivier [16]. As seen, the augmentation ratio f_* shows a strong dependence on *p/e* and Reynolds number. The values of f_* decrease with the increase of *p/e* and there are different variations of f_* within the ranges *p/e* = 6.7-9.0 and *p/e* = 10.0-15.0. In the first range, f_* experiences two maxima in the curve $f_* = f(\mathrm{Re}, p/e)$, for Re~$2\cdot10^3$, and Re~$5\cdot10^3$, and two minima for Re~$3\cdot10^3$ and Re~$6\cdot10^3$, whereas in the second range, *p/e* = 10.0-15.0, the curve of f_* experiences only one maximum for Re~$2\cdot10^3$ and one minimum for Re~$3\cdot10^3$. Afterwards the curves gradually slowly increase with the increase of Reynolds number. This different behavior can be explained by the different nature of the flow between the ribs, a boundary-layer with or without separation, and reattachment.

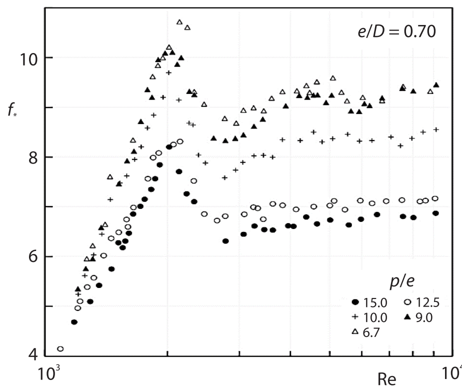

Figure 5. The variation of f_* with Re

Figures 6 and 7 show the variation of $\mathrm{Nu_a}$ with Reynolds and Prandtl numbers for *p/e* = 6.7 and 15.0 (similar images have been obtained for the rest of *p/e*). Similarly to f_a, different variations of $\mathrm{Nu_a}$ with Reynolds and Prandtl numbers are observed in the ranges *p/e* = 6.7-9.0 and *p/e* = 10.0-15.0. In this regard, two simple correlations can also be developed for Re > $3\cdot10^3$. In the range *p/e* = 6.7-9.0:

$$\mathrm{Nu_a} = 0.060\,\mathrm{Re}^{0.70}\,\mathrm{Pr}^{0.90}(p/e)^{-0.17} \tag{4}$$

with RMS deviation of 4.6% (144 experimental points), fig. 8. The relative deviations of all 144 experimental points from the correlation, eq. (4), are in the range ±10%.

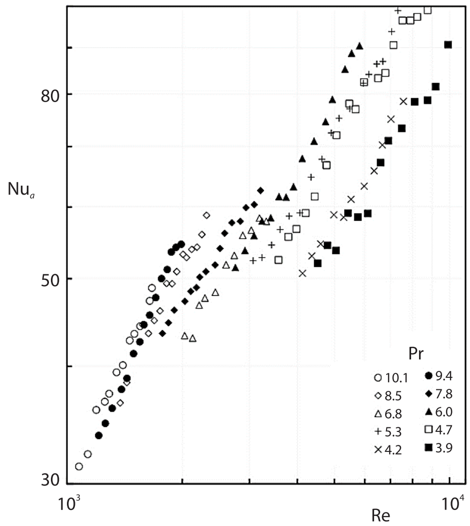

Figure 6. The variation of $\mathrm{Nu_a}$ with Re for different Pr (*p*/*e* = 6.7)

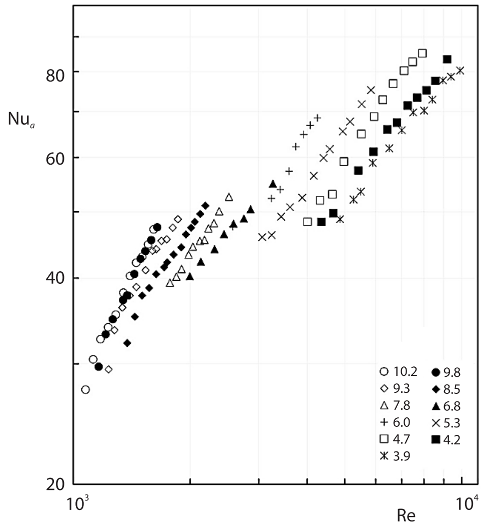

Figure 7. The variation of $\mathrm{Nu_a}$ with Re for different Pr (*p*/*e* = 15.0)

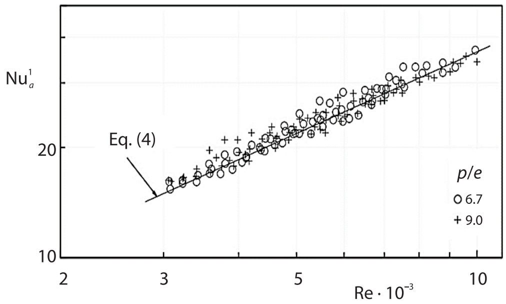

Figure 8. The variation of $\mathrm{Nu_a^1} = \mathrm{Nu_a Pr^{-0.90}}(p/e)^{0.17}$ with Re

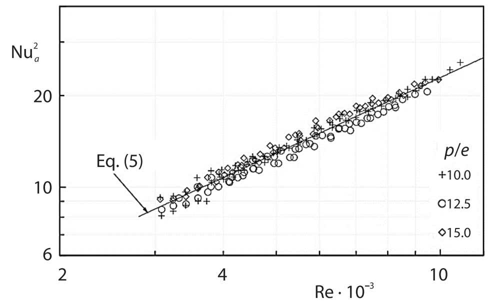

Figure 9. The variation of $\mathrm{Nu_a^2} = \mathrm{Nu_a Pr^{-1.124}}(p/e)^{0.096}$ with Re

In the range *p*/*e* = 10.0-15.0:

$$\mathrm{Nu_a} = 0.0115\,\mathrm{Re}^{0.825}\,\mathrm{Pr}^{1.124}(p/e)^{-0.096} \tag{5}$$

with RMS deviation of 4.2% (186 experimental points) for *p*/*e* = 10.0-15.0, fig. 9. The relative deviations of all 186 experimental points from the correlation, eq. (5), are in the range ±10%.

The heat transfer augmentation is defined by the ratio $\mathrm{Nu_*} = \mathrm{Nu_a}/\mathrm{Nu_s}$ at the same Reynolds and Prandtl numbers. The maximum value of this ratio $\mathrm{Nu_*^{max}}$ appears at $\mathrm{Re} \sim 1.8 \cdot 10^3$ and depends on Prandtl number and *p*/*e*. Figure 10 shows $\mathrm{Nu_*^{max}}$ for the wire-coil inserts studied.

It is obvious that the most effective relative pitch is close to *p*/*e* = 10 and with the increase of Prandtl number the $\mathrm{Nu_*^{max}}$ also increases. Using eqs. (4) and (5), and with the variation of Nusselt with Prandtl number for the smooth tube, Nu~$Pr^{0.42}$ [12, 13], the heat transfer augmentation ratio can be presented in the form:

$$\mathrm{Nu}_* \sim f(\mathrm{Re})\,\mathrm{Pr}^{0.48}(p/e)^{-0.17} \tag{6}$$

for p/e = 6.7-9.0, and $10^3 < \mathrm{Re} < 10^4$, and

$$\mathrm{Nu}_* \sim f(\mathrm{Re})\,\mathrm{Pr}^{0.70}(p/e)^{-0.096} \tag{7}$$

for p/e = 10.0-15.0, and $10^3 < \mathrm{Re} < 10^4$.

Figures 11 and 12 show the variation of Nu_*^+ with Reynolds number for two regions p/e = 6.7-9.0 and p/e = 10.0-15.0. As seen all points collapse on two similar curves $\mathrm{Nu}_*^+ = f(\mathrm{Re})$.

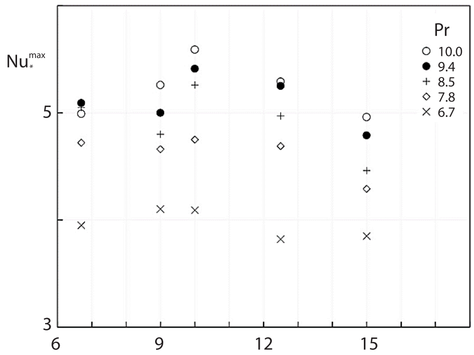

Figure 10. The variation of $\mathrm{Nu}_*^{\mathrm{max}}$ with p/e for Pr = 6.7-10.0

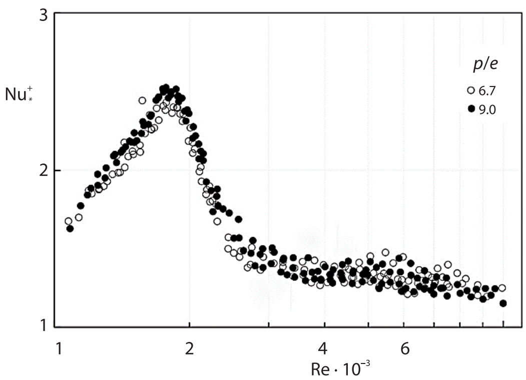

Figure 11. The variation off $\mathrm{Nu}_*^+ = \mathrm{Nu}_*\mathrm{Pr}^{-0.48}(p/e)^{0.17}$ with Re

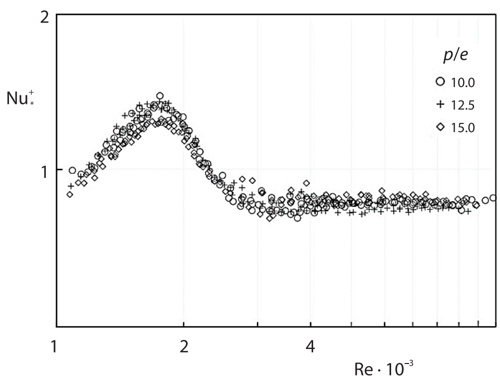

Figure. 12. The variation of $\mathrm{Nu}_*^+ = \mathrm{Nu}_*\mathrm{Pr}^{-0.70}(p/e)^{0.096}$ with Re

Performance evaluation

Many performance evaluation criteria (PEC) have been developed for evaluating the performance of heat exchangers, based on the first law, Yilmaz *et al.* [17], or criteria based on the Second law of thermodynamics, Yilmaz *et al.* [18]. A real assessment of the benefit can be obtained only by the PEC developed by Webb [19]. The evaluation of the benefit by Second law analysis has been proposed by Bejan [20] in developing the entropy generation minimization method, which has been further extended by Zimparov [21, 22]. A recent critical review on the use of PEC has been presented by Zimparov *et al.* [14].

In this regard, following Webb [19], the most important equation is that for the relative overall heat conductance:

$$(UA)_* = \frac{1+\beta_\mathrm{s}}{\mathrm{St}_*^{-1}\left(f_* P_*^{-1} A_*^{-2}\right)^{1/3} + \beta A_*^{-1}} \tag{8}$$

where β and β_s the are thermal resistances, $P_* = P_\mathrm{a}/P_\mathrm{s}$, $A_* = A_\mathrm{a}/A_\mathrm{s}$, $\mathrm{St}_* = \mathrm{St}_\mathrm{a}/\mathrm{St}_\mathrm{s}$. When the objective is increased heat duty, $Q_* = Q_\mathrm{a}/Q_\mathrm{s} > 1$:

$$Q_* = W_* \varepsilon \Delta T_i^* \tag{9}$$

where $W_* = W_a/W_s$, $\varepsilon_* = \varepsilon_a/\varepsilon_s$, $\Delta T_i^* = \Delta T_{i,a}/\Delta T_{i,s}$, Webb [19]. In this study, we consider only the case FG-1a, where the objective is the increased heat duty, $Q_* > 1$, for an existing heat exchanger, where the smooth pipes are furnished with wire-coil inserts.

The case FG-1a seeks $Q_* > 1$ and $N_{s,a} < 1$, for $W_* = 1$, $A_* = 1$. As a consequence the pumping power will increase, $P_* > 1$. If the entering fluid temperature differences are fixed, $\Delta T_i = 1$, eq. (9) gives $Q_* = \varepsilon_*$ and this is the benefit that can be obtained. If $R_{ext} = 0$, and $\beta = \beta_s = 0$, eq. (8) yields:

$$(UA)_* = \mathrm{St}_* \tag{10}$$

Equation (10) gives the maximum increase of the overall thermal conductivity of the heat exchanger. In this case, $N_{s,a}$, [14, 22], becomes:

$$N_{s,a} = \frac{1}{1+\phi_o}\left(\frac{Q_*^2}{\mathrm{Nu}_*}\frac{T_{o,s}}{T_{o,a}} + \phi_o \frac{f_*}{D_*^5}\right) \tag{11}$$

Figure 13 presents the variation of Q_*, with Reynolds and Prandtl numbers. The first curve (at the top) presents the maximum thermal conductivities $(UA)_*^{max} \equiv (hA)_* = \mathrm{Nu}_*$. As seen, the maximum value of Nu_* reaches almost 5.5 at $\mathrm{Re} \approx 1.8 \cdot 10^3$ and Pr = 10.0. However, this is not the real benefit. The second curve (in the middle) presents the maximum possible increase of heat flow, Q_*^{max} (the case for $R_{ext} = 0$). The maximum possible profit is $Q_*^{max} = 3.0$, and can be achieved at $\mathrm{Re} \approx 1.8 \cdot 10^3$ and Pr = 10.0. In reality, since $R_{ext} \neq 0$, the real benefit is much smaller. The third curve (in the bottom) presents the real profit that has been obtained, $Q_*^{real} \approx 1.70$, for $\mathrm{Re} \approx 1.8 \cdot 10^3$ and Pr = 10.0.

Figure 14 presents the variation of $N_{s,a}$ (upper part of the figure) and $N_s^+ = N_{s,a}/Q_*$ (lower part) with Reynolds number, only for $Q_* = Q_*^{real}$ ($R_{ext} \neq 0$), since for $Q_* = Q_*^{max}$ ($R_{ext} = 0$) $N_{s,a} > 1$ and the objective $N_{s,a} < 1$ has not been achieved. This is due to the greater increase of the heat flow which increases the entropy generation due to heat flow, N_T and consequently $N_{s,a}$. However, for a real counter flow heat exchanger $R_{ext} \neq 0$, $Q_*^{real} < Q_*^{max}$, and particularly in this study, the two objectives $Q_* > 1$ and $N_{s,a} < 1$ have been achieved, despite the increase in pumping power, $P_* > 1$.

The variation of N_s^+ (lower part of fig. 14) with Reynolds number shows a minimum of $N_s^+ \approx 0.3$ for $\mathrm{Re} \approx 1.8 \cdot 10^3$. This value can be used for comparison with the performance of other heat transfer enhancement techniques.

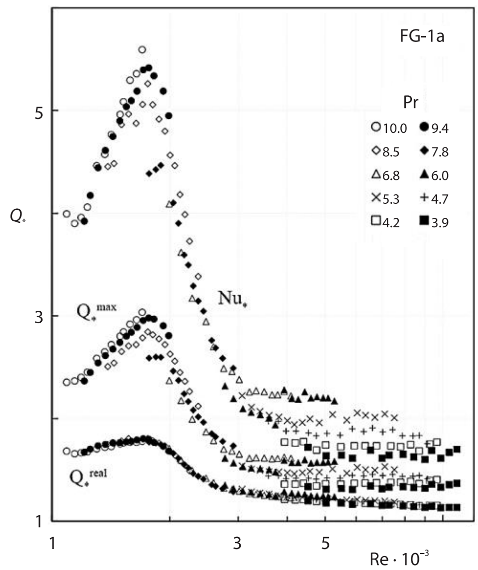

Figure 13. The variation of Q_* with Re, p/e = 10.0

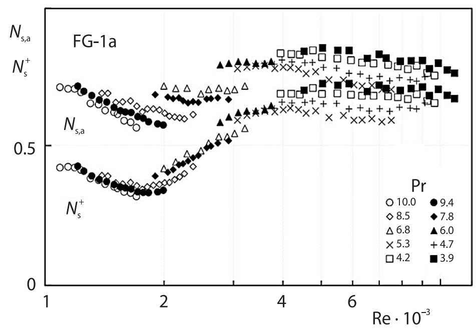

Figure 14. The variation of $N_{s,a}$ and N_s^+ with Re and Pr for Q_*^{real}, p/e = 10.0

Figure 15 presents the variation of N_s^+ with Reynolds and Prandtl numbers (6.8 < Pr < 10.0) for different *p*/*e*. As seen:

- all curves have a minimum around Re ≈ $1.8 \cdot 10^3$,
- for Re < $2.3 \cdot 10^3$, the best performance possesses the wire-coil insert with *p*/*e* = 10.0, whereas for Re > $2.3 \cdot 10^3$, the wire-coil inserts with *p*/*e* = 6.7, 9.0, and 10.0 perform with equal effectiveness, and
- when *p*/*e* > 10.0 the effectiveness of the wire-coil inserts gradually decreases.

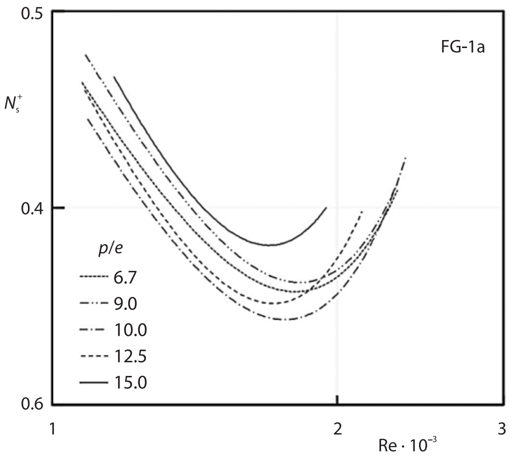

Figure 15. The variation of N_s^+ ($Q_* = Q_*^{\mathrm{real}}$) with Re for different *p*/*e*, (6.8 < Pr < 10.0)

Conclusions

An experimental study has been performed to find out the influence of the pitch of wire-coil inserted in a smooth tube, for transition and low turbulent flow regimes. The maximum and real benefits have been assessed for the case FG-1a. The results can be summarized.

- For Re > $3 \cdot 10^3$, the increase of *f* and Nusselt number can be presented by simple power correlations for *p*/*e* = 6.7-9.0 and *p*/*e* = 10.0-15.0.
- The ratios $f_* = f(\mathrm{Re}, p/e)$ and $\mathrm{Nu}_* = f(\mathrm{Re}, \mathrm{Pr}, p/e)$ experienced maximum for Re ≈ $1.8 \cdot 10^3$.
- Correlations in the form $N_s^+ = f(\mathrm{Re})$ can be obtained.
- The greatest benefit can be achieved by the use of pitch of wire-coil insert *p*/*e* = 10.0, and new design heat exchanger.

Acknowledgment

This study has been supported by the European Regional Development Fund within the OP *Science and Education for Smart Growth 2014-2020*, Project No. BG-05M2OP001-1.002-0023.

Nomenclature

A – heat transfer surface area, [m^2]
D – tube diameter, m
e – rib height (wire diameter), [m]
f – Fanning friction factor
h – heat transfer coefficient, [Wm^{-2}K^{-1}]
Nu – Nusselt number
N_s – number of entropy production units
$N_{s,a}$ – augmentation entropy generation number
P – pumping power, [W]
p – pitch of wire-coil, [m]
Pr – Prandtl number
Q – heat transfer rate, [W]
Re – Reynolds number
St – Stanton number
T – temperature, [K]
ΔT – temperature difference, [K]
U – overall heat transfer coefficient, [Wm^{-2}K^{-1}]
W – mass-flow rate in heat exchanger, [kgs^{-1}]

Greek symbols

β – sum of thermal resistances, [m^{2}KW^{-1}]
ε – heat exchanger thermal effectiveness
ϕ_o – irreversibility distribution ratio

Subscripts

a – augmented tube
i – inside
o – outside
s – smooth tube

References

[1] Webb, R., Kim N., *Principles of Enhanced Heat Transfer*, 2nd ed., Taylor and Francis Group, New York, USA, 2005

[2] Garcia, A, *et al.*, Experimental Study of Heat Transfer Enhancement with Wire Coil Inserts in Laminar-Transitional-Turbulent Regimes at Different Prandtl Numbers, *Int. J. Heat Mass Transfer*, *48* (2005), 21-22, pp. 4640-4651
[3] Garcia, A., *et al.*, Enhancement of Laminar and Transitional Flow Heat Transfer in Tubes by Means of Wire Coil Inserts, *Int. J. Heat Mass Transfer*, *50* (2007), 15-16, pp. 3176-3189
[4] Martinez, D. S., *et al.*, Heat Transfer Enhancement of Laminar and Transitional Newtonian and Non-Newtonian Flows in Tubes with Wire Coil Inserts, *Int. J. Heat Mass Transfer*, *76* (2014), Sept., pp. 540-548
[5] Kumar A., Prasad, B. N., Investigation of Twisted Tape Inserted Solar Water Heaters – Heat Transfer, Friction Factor and Thermal Performance Results, *Ren. Energy*, *19* (2000), 3 pp. 379-398
[6] Jaisankar, S., *et al.*, Experimental Studies on Heat Transfer and Friction Factor Characteristics of Forced Circulation Solar Water Heater System Fitted with Helical Twisted Tapes, *Solar Energy*, *83* (2009), 11, pp. 1943-1952
[7] Jaisankar, S., *et al.,* Studies on Heat Transfer and Friction Factor Characteristics of Thermosiphon Solar Water Heating System with Helical Twisted Tapes, *Energy*, *34* (2009), 9, pp. 1054-1064
[8] Jaisankar, S., *et al.*, Experimental Investigation of Heat Transfer and Friction Factor Characteristics of Thermosiphon Solar Water Heater System Fitted with Spacer at the Trailing Edge of Left-Right Twisted Tapes, *Energy Conv. Mang.*, *50* (2009),10, pp. 2638-2649
[9] Ananth, J., Jaisankar, S., Experimental Studies on Heat Transfer and Friction Factor Characteristics of Thermosiphon Solar Water Heating System Fitted with Regularly Spaced Twisted Tape with Rod and Spacer, *Energy Conv. Mang*., *73* (2013), Sept., pp. 207-213
[10] Duffie, J. A., Beckman, W. A., *Solar Engineering of Thermal Processes*, 3rd ed., John Wiley AND Sons, Hoboken, N. J., USA,2006.
[11] Garcia, A., *et al.*, Experimental Study of Heat Ttransfer Enhancement in Flat-Plate Solar Water Collector with Wire-Coil Inserts, *App. Therm. Eng*., *61* (2013), 2, pp. 461-468
[12] Zimparov, V. D., *et al.*, Transitional Heat Transfer and Pressure Drop in Plain Horizontal Tubes*, Int. Rev. Chem. Eng*., *7* (2015), 2, pp. 37-44
[13] Zimparov, V. D., *et al.*, Transitional Heat Transfer and Pressure Drop in Plain Horizontal Tubes – Revised Study, *Int. Rev. Chem. Eng.*, *9* (2017), 1, pp. 1-7
[14] Zimparov, V. D., *et al.*, Benefits from the Use of Enhanced Heat Transfer Surfaces in Heat Exchanger Design: A Critical Review of Performance Evaluation, *Journal Enh. Heat Transfer*., *23* (2016), 5, pp. 371-393
[15] Vicente, P. G., *et al.*, Heat Transfer and Pressure Drop for Low Reynolds Turbulent Flow in Helically Dimpled Tubes, *Int. J. Heat Mass Transfer*, *45* (2002), 3, pp.543-553
[16] Olivier, J. A., Single-Phase Heat Transfer and Pressure Drop of Water Inside Horizontal Circular Smooth and Enhanced Tubes with Different Inlet Configurations Flow Regime, Ph. D. thesis, University of Pretoria, Pretoria, South Africa, 2009
[17] Yilmaz, M., *et al*, Performance Evaluation Criteria for Heat Exchangers Based on First Law Analysis, J*ournal Enh. Heat Transfer*, *12* (2005), 2, pp. 121-157
[18] Yilmaz, M., *et al*, Performance Evaluation Criteria for Heat Exchangers Based on Second Law Analysis, *Exergy Int. J*., *1* (2001), 4, pp. 278-294
[19] Webb, R. L., Performance Evaluation Criteria for Use of Enhanced Heat Exchanger Surfaces in Heat Exchanger Design, *Int. J. Heat Mass Transfer*, *24* (1981), 4, pp. 715-726
[20] Bejan, A., *Entropy Generation through Heat and Fluid-Flow,* Wiley, New York, USA, 1982
[21] Zimparov, V., Extended Performance Evaluation Criteria for Enhanced Heat Transfer Surfaces: Heat Transfer Through Ducts with Constant Wall Temperature, *Int. J. Heat Mass Transfer*, *43* (2000), 1, pp. 3137-3155
[22] Zimparov, V., Extended Performance Evaluation Criteria for Enhanced Heat Transfer Surfaces: Heat Transfer through Ducts with Constant Heat Flux, *Int. J. Heat Mass Transfer*, *43* (2001), 1, pp. 3137-3155

Paper submitted: December 6, 2021
Paper revised: April 2, 2022
Paper accepted: April 8, 2022